

# Synthetic wavelength scanning interferometry for 3D surface profilometry with extended range of height measurement using multi-color LED light sources

Priyanka Mann<sup>1</sup>, Vishesh Dubey<sup>1,2</sup>, Azeem Ahmad<sup>2</sup>, Ankit Butola<sup>2</sup> & Dalip Singh Mehta<sup>1</sup>

<sup>1</sup>*Applied Optics and Bio-photonics Laboratory, Indian Institute of Technology Delhi, India*

<sup>2</sup>*Department of Physics and Technology, UiT The Arctic University of Norway, Tromsø, Norway*

\*Corresponding author: [mehtads@physics.iitd.ac.in](mailto:mehtads@physics.iitd.ac.in)

## Abstract

We report a three-dimensional surface profilometry with extended range of height measurement using synthetic wavelength scanning interferometry without any tunable filters, wavelength-tuning lasers, or grating elements. Here, we have used inexpensive multiple color light emitting diodes (LEDs) and operate them sequentially one by one or combination of two or more colors simultaneously to generate synthetic wavelength light source for illumination. Multiple color LED light source was synthesized and entire visible range from violet to deep red color was covered. A wide range of synthetic wavelengths were obtained. Experiments were performed on industrial objects and interferograms were recorded using Mirau type interferometer. Five step phase shifting algorithm was used to recover the phase maps which can be further utilized for 3D height measurement of the specimen. A simple phase subtraction method was used to reconstruct the phase map at synthetic wavelength thus extending the range of step-height measurement. The present system provides extended range of height measurement from sub-wavelength to tens of wavelengths. Experimental results of 3D-surface profile measurements of a Si-IC chip and a standard step object are presented. The present system does not require expensive multiple color filters or any wavelength scanning mechanism along with a broadband light source.

**Keywords:** Synthetic wavelength, Multi-color LED, extended range, step-height measurement.

## 1. Introduction

Optical interferometric techniques have played an important role in three-dimensional surface profilometry or step-height measurements of micro and nanostructures of opto-electronic components and other industrial objects. These optical techniques are wide field, non-contact, non-invasive, high-precision, and high-resolution. Some of these methods were used in heterodyne interferometry [1] and phase-shifting interferometry [2,3] which offer sub-nanometric resolution. However, for complex discontinuous objects with large step-height and discontinuities, these techniques suffer from modulo- $2\pi$  phase ambiguity problem which limits the maximum measurable range to half the wavelength. A range of other techniques were developed to extend the range of step-height measurement beyond  $2\pi$ -phase ambiguity problem. Among these methods, optical coherence scanning microscopy [4,5], three-dimensional sensing by coherence radar [6], scanning white light interferometry [7], and wavelength scanning interferometry [8-13] are the most important. These techniques are well established for 3D-surface profilometry of both specular and diffuse objects with large range of measurement beyond  $2\pi$ -phase ambiguity problem. But some of these techniques require mechanical scanning of reference mirror, piezo-controlled object stage or high-precision

mechanical stages for phase-shifting and coherence scanning, and this scan tends to take relatively more time, but it has its own advantages also. The reflected light from the edges of the step will surely diffract and have some influences but in phase shifting algorithm the expression for phase includes some addition and subtraction of intensity terms (interferograms) which are further divided to evaluate the phase and it will suppress or minimises the diffraction effects if exists. And also it depends upon the coherence length of the source i.e., unwanted lighting effects (diffraction in our case) are minimum for low coherent light sources (LED, white light source). Further, in the phase shifting analysis method any undesired and unwanted effects i.e., noise is cancelled out.

The wavelength scanning interferometry [14,15] is a non-mechanical scanning technique and has potential for absolute surface measurements. This leads to a wide range of measurements and the upper limit is determined by the maximum wavelength scanning range and the spectral width of the tunable light source.

So far various kinds of light sources have been used, such as, mode-hop free external cavity diode laser [8-11], and Ti-Sapphire laser system with a suitable tunable filter [12] for successful demonstration of wavelength scanning interferometry. Recently, some non-mechanical scanning and convenient solutions has been developed for wavelength scanning systems such as, a super-luminescent diode (SLD) as a broad-band light source with liquid-crystal Fabry-Perot interferometer (LC-FPI) [13-16], wavelength scanning device and its transmission spectrum can be tuned by applying a low voltage; thus, no mechanical movement of optical components is required. Another combination comprises a SLD as a broad-band light source and an acousto-optic tunable filter [17-18] as a wavelength tuning device. Both the systems are simple and easy to operate. Another method to measure the step-height with extended range is a two-wavelength interferometry [19-23], in which two lasers with different peak wavelength are interfered and a synthetic wavelength is generated. The range of step height measurement can be extended beyond  $2\pi$ -phase ambiguity with this method. Multiple wavelength interferometry [24-29] using multiple color lasers, has been also used to obtain the range of synthetic wavelength for the measurement of extended step height. Although proposed systems can provide wide wavelength-scanning range and therefore provides high-resolution and large dynamic range in step-height measurement, but these systems are bulky, expensive and requires precise alignment therefore, inconvenient for industrial purposes. Further, the laser-based systems lead to speckle patterns during rough objects measurements. The key requirement is a multiple wavelength light source which is low cost, compact in size, field portable and a large range of synthetic wavelengths can be generated for a scalable range of step-height measurement [30-33].

The interplay between the temporal and axial spatial coherence plays a major role in interference microscopes but more prominently in case of off-axis linnik type interferometric microscope as compared to nearly common path interferometers like Taylor and Mirau type interferometric microscopes [34,35].

The longitudinal coherence length of a light source generally depends on both the angular frequency as well as the temporal frequency spectrum as given below

$$L_c = \left[ \frac{2 \sin^2\left(\frac{\theta}{2}\right)}{\lambda_0} + \frac{\Delta\lambda}{\lambda_0^2} \cos^2\left(\frac{\theta}{2}\right) \right]^{-1} \quad [1]$$

Where  $\lambda_0$  is the central peak wavelength and  $\theta$  and  $\Delta\lambda$  are half of the spectral and temporal width of the illuminating source. Depending on the size of illuminating light source one of the terms in the above expression becomes dominant. When the source size is small (point source) the coherence length can be given by the second term, the frequency spectrum term whereas if the source size is large (extended), the temporal spectral width is narrow then the coherence

length is given by the angular frequency term. Hence for narrow temporal spectral width of the source the coherence length is given by

$$L_c = \frac{2 \sin^2\left(\frac{\theta}{2}\right)}{\lambda_0} \quad [2]$$

Here, the axial resolution ( $\frac{L_c}{2}$ ) is dominated by the longitudinal spatial coherence as compared to the temporal coherence length.

Here we report a synthetic wavelength scanning interferometry using inexpensive multiple color programmable LED light source which can be tuned electronically, and it doesn't generate speckle patterns during measurements of rough object. Multiple color LEDs over the entire visible range with narrow spectral bandwidth were assembled into a synthesized small light source. Since the spectral widths of LEDs are few tens of nanometres as shown in Figure 1(b) which is inversely proportional to the coherence length of the illuminating source. So, the coherence length of LEDs is much smaller as compared to that of lasers which can affect the interferogram signals, but these factors can be compensated by the fact that our proposed Mirau objective based interferometric system is compact and nearly common path which can provide the interferograms very fast within the coherence length of the illuminating source. Although low coherence or large spectral width of LEDs has limited the height measurements up to some few microns but also it provides speckle free imaging as compared to lasers which are highly coherent and suffers from speckles and spurious fringes which can be further removed but again it makes the system more complex. The multi-color LED light source was designed and operated sequentially one-by-one or combination of two or more colors at a time as a wavelength scanning light source. This multiple wavelength light source was coupled with a Mirau-interferometric microscope. Mirau interferometric objective lens is a nearly common path interferometer which can be operated both in bright field and interferometric imaging i.e., by slightly adjusting the optical path length, interference can be obtained. This Mirau objective lens is a standard objective corrected for multiple colors [36-38]. It also provides speckle free imaging due to the low spatial and temporal coherence of the source as compared to the monochromatic source (laser) which leads to the formation of speckles and spurious fringes which degrades the quality of the interferograms. Phase shifting interferometry combined with phase-subtraction is used to reconstruct the phase map at synthetic wavelengths. A wide range of synthetic wavelengths were obtained using the multiple color LED light source thus a large range of extended step-height measurement from a simple and inexpensive light source is achieved. Experimental results of 3D-surface profile measurement of a standard object are presented for the proof of concept. This synthesized system can be used for surface profiling of various industrial objects over large field of view (FOV).

## 2. Wavelength scanning interferometry using multi-color LED light source

A small wavelength light source is one of the major advantages of optical interferometry and at the same time, it has its own disadvantages also. The sensitivity of a single wavelength interferometric measurement is very high, but the dynamic range is limited due to the short wavelength of light. One of the solutions to this problem is to perform the measurements at multiple wavelengths and then compare the measurement results for the different wavelengths to determine the actual structure of the specimen. By combining multiple-wavelength interferometry with phase-shifting techniques became very powerful tool for extending the range of measurements of step-height objects with high precision and phase sensitivity [27,36]. Five step phase shifting algorithm along with color fringe analysis were used to reconstruct the

phase map and hence the height profile of the specimen. Five phase shifted 2D interferograms can be represented by the following expressions [39-41]

$$I_{1,i}(x, y, \lambda_i) = I_0(x, y, \lambda_i)[1 + V_i\gamma(z)\cos\{\phi_i(x, y, \lambda_i) - 2\delta_i\}] \quad [3]$$

$$I_{2,i}(x, y, \lambda_i) = I_0(x, y, \lambda_i)[1 + V_i\gamma(z)\cos\{\phi_i(x, y, \lambda_i) - \delta_i\}] \quad [4]$$

$$I_{3,i}(x, y, \lambda_i) = I_0(x, y, \lambda_i)[1 + V_i\gamma(z)\cos\{\phi_i(x, y, \lambda_i)\}] \quad [5]$$

$$I_{4,i}(x, y, \lambda_i) = I_0(x, y, \lambda_i)[1 + V_i\gamma(z)\cos\{\phi_i(x, y, \lambda_i) + \delta_i\}] \quad [6]$$

$$I_{5,i}(x, y, \lambda_i) = I_0(x, y, \lambda_i)[1 + V_i\gamma(z)\cos\{\phi_i(x, y, \lambda_i) + 2\delta_i\}] \quad [7]$$

Where  $i$  stands for different color LEDs:  $i = D, R, A, G, B$  and  $V$  for deep red, red, amber, green, blue and violet.  $I_0(x, y, \lambda_i)$  is the background intensity,  $V_i$  is the fringe contrast and  $\gamma(z)$  is the coherence envelop of light source and defined as  $\gamma(z) = \exp\left[-2\pi\left(\frac{z - z_0}{l_c}\right)^2\right]$  with coherence length  $l_c$ .

In phase shifting interferometry (PSI), a time varying phase shift  $\delta_i$  is introduced between the sample arm and the reference arm by moving the reference mirror using Piezo electric transducer (PZT). This specific movement corresponds to an exact phase shift of  $\frac{\pi}{2}$  only for a single wavelength. In our system PZT is calibrated for green wavelength ( $\lambda = 532$  nm). The phase shift between the adjacent interferograms is different from  $\frac{\pi}{2}$  for wavelengths other than green so an additional term  $(n - 1)\delta_i$  is introduced in the interferogram intensity equation as follows:

$$I_{1,i}(x, y, \lambda_i) = I_0(x, y, \lambda_i)[1 + V_i\gamma(z)\cos\{\phi_i(x, y, \lambda_i) + (n - 1)\delta_i\}] \quad [8]$$

For wavelengths corresponding to which  $\delta_i$  is not exactly  $\frac{\pi}{2}$ , it can be evaluated by least square approximations given by  $\delta_i = \frac{\lambda_i}{\lambda_1} \frac{\pi}{2}$  where  $\lambda_1$  is the wavelength for which PZT is calibrated (green in our case) and  $\lambda_i$  is for which  $\delta_i$  has to be evaluated. Further the expression for phase retrieval is modified by an addition term of  $\sin\delta_i$  which is 1 for PZT calibrated wavelengths ( $\delta_i = \frac{\pi}{2}$ ) and has different values for other wavelengths [42-43]. The phase of the specimen can be extracted using five phase shifted interferograms as follows [37]

$$\phi_i(x, y, \lambda_i) = \tan^{-1} \left[ \sin\delta_i \frac{2(I_{4,i}(x, y, \lambda_i) - I_{2,i}(x, y, \lambda_i))}{I_{1,i}(x, y, \lambda_i) - 2I_{3,i}(x, y, \lambda_i) + I_{5,i}(x, y, \lambda_i)} \right] \quad [9]$$

Further two-wavelength or synthetic wavelength interferometry is achieved with the present multi-color LED light source by switching on two or three colors simultaneously. This can be done by using two methods; (a) phase subtraction method and (b) two wavelengths can be switched on simultaneously. We have used the first method in the present study where individual interferograms are recorded by sequentially operating the multi-color LED light source. The phase map corresponding to each interferogram was reconstructed using aforementioned method. Phase subtraction method was then used to reconstruct the phase at synthetic wavelength using the following expression [44,45]:

$$\Delta\Phi(x, y) = \phi_1(x, y, \lambda_1) - \phi_2(x, y, \lambda_2) = 2\pi\left(\frac{1}{\lambda_1} - \frac{1}{\lambda_2}\right)OPD = \frac{2\pi}{\Lambda}OPD \quad [11]$$

$\Delta\Phi(x, y)$  is the phase map at synthetic wavelength  $\Lambda = \frac{\lambda_1\lambda_2}{\text{abs}[\lambda_1 - \lambda_2]}$ . The recovered phase of the specimen has the information of the height profile  $h(x, y)$  of the specimen which can be extracted using following formula [36,37]:

$$h(x, y) = \frac{\Lambda}{4\pi}\Delta\Phi(x, y) \quad [12]$$

Figure 1 (a) shows the spectral distributions of multiple color LEDs, which were operated sequentially or in combination of two-colors simultaneously to obtain the synthetic wavelengths.

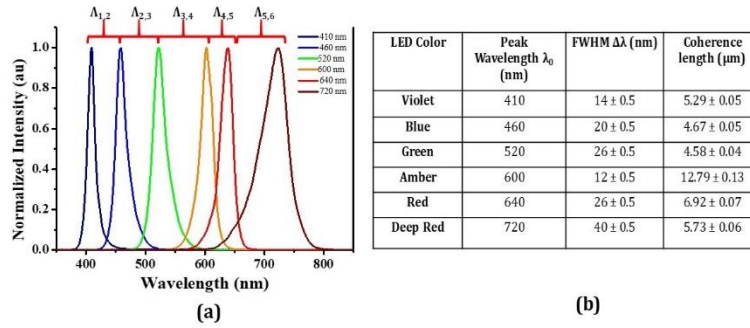


**Fig.1** (a): Spectral distribution of multi-color LED light sources, (b) Bandwidth and coherence length of multicolor LEDs.

From Fig.1 (a) we can see that a wide range of synthetic wavelengths can be achieved by different combinations of the individual wavelengths. But this range is not limited only up to five synthetic wavelengths, rather we can achieve a large number of synthetic wavelength combinations. This is achieved by switching on  $\lambda_1$  first and then sequentially switching on  $\lambda_2, \lambda_3, \lambda_4, \lambda_5,$  and  $\lambda_6,$  respectively, and so on. In this way we can achieve a large number of synthetic wavelengths and range of step height measurement in increasing order using the above-mentioned LED light source. With the present system a total 15 combinations of synthetic wavelengths can be achieved within the coherence length of the LED light source mentioned in Fig.1(b). Since the spectral profiles of all the LEDs are Gaussian, therefore for Gaussian spectral profile the following formula has been used for computing the coherence length

$$l_c = \frac{2 \ln 2}{\pi} \frac{\lambda^2}{\Delta\lambda} = 0.44 \frac{\lambda^2}{\Delta\lambda} \quad [10]$$

Where  $\Delta\lambda$  is the full width half maxima (FWHM) and  $\lambda$  is the peak wavelength of the illuminating source. For all the low coherent light sources with gaussian spectral profile the above formula has been used [46]. Table-1 shows the extended range of height measurement from  $0.6 \mu\text{m}$  up to  $2.24 \mu\text{m}$ . Therefore, this method is suitable for 3D-profilometry of complex discontinuous objects with large step-height and discontinuities. The synthetic wavelength scanning interferometry can be operated on ascending or descending order with the appropriate choice of two-color LEDs switched on at a time as can be seen from Table-1. The same can also be obtained by phase subtraction method by using the individual interferograms. The illumination with multiple or two LEDs switched on either simultaneously or individually doesn't matter both the approaches can be utilised to achieve the synthetic wavelength approach

which can be further employed to eliminate the phase ambiguity issues which occurs in step like object height measurements. Basically, the multiple illumination is concerned with the extension of range of height measurement. The range of height measurement depends upon the coherence length of the source, so the LED based source is capable of few  $\mu\text{m}$  height measurements.

**Table 1: Range of synthetic wavelength and height measurement using multicolor LEDs**

Wavelength( $\lambda$ )	Value (nm)	Synthetic wavelength range $\Lambda$	Extended range of height measurement ( $\Lambda/2$ )
$\lambda_1$	460	$\Lambda_{1,6} = \frac{\lambda_1 \lambda_6}{ \lambda_1 - \lambda_6 } = 1.274 \mu\text{m}$	0.637 $\mu\text{m}$
$\lambda_2$	520	$\Lambda_{1,5} = \frac{\lambda_1 \lambda_5}{ \lambda_1 - \lambda_5 } = 1.635 \mu\text{m}$	0.8175 $\mu\text{m}$
$\lambda_3$	560	$\Lambda_{2,6} = \frac{\lambda_2 \lambda_6}{ \lambda_2 - \lambda_6 } = 1.872 \mu\text{m}$	0.936 $\mu\text{m}$
$\lambda_4$	600	$\Lambda_{1,4} = \frac{\lambda_1 \lambda_4}{ \lambda_1 - \lambda_4 } = 1.971 \mu\text{m}$	0.9855 $\mu\text{m}$
$\lambda_5$	640	$\Lambda_{1,3} = \frac{\lambda_1 \lambda_3}{ \lambda_1 - \lambda_3 } = 2.576 \mu\text{m}$	1.288 $\mu\text{m}$
$\lambda_6$	720	$\Lambda_{2,5} = \frac{\lambda_2 \lambda_5}{ \lambda_2 - \lambda_5 } = 2.773 \mu\text{m}$	1.3865 $\mu\text{m}$
		$\Lambda_{4,6} = \frac{\lambda_4 \lambda_6}{ \lambda_4 - \lambda_6 } = 3.6 \mu\text{m}$	1.8 $\mu\text{m}$
		$\Lambda_{2,4} = \frac{\lambda_2 \lambda_4}{ \lambda_2 - \lambda_4 } = 3.9 \mu\text{m}$	1.95 $\mu\text{m}$
		$\Lambda_{1,2} = \frac{\lambda_1 \lambda_2}{ \lambda_1 - \lambda_2 } = 3.986 \mu\text{m}$	1.993 $\mu\text{m}$
		$\Lambda_{3,5} = \frac{\lambda_3 \lambda_5}{ \lambda_3 - \lambda_5 } = 4.48 \mu\text{m}$	2.24 $\mu\text{m}$
and so on.....			

The depth of field (DOF) of the objective depends upon the Numerical aperture (NA) of the objective and the wavelength  $\lambda$  of illumination as follows [47]:

$$\text{Depth of Field} = \lambda \frac{\sqrt{1-(NA)^2}}{(NA)^2} \quad [11]$$

In the present system we have used a wide range of wavelength source so the depth of field of the objective varies accordingly depending on the wavelength of illuminating source. Table-2 represent the range of depth of field with the wavelength of illuminating source (NA = 0.55) as follows

**Table 2: Range of depth of field with the wavelength of illuminating source**

Wavelength( $\lambda$ )	Value (nm)	Depth of field (DOF)
$\lambda_1$	460	1.270 $\mu\text{m}$
$\lambda_2$	520	1.435 $\mu\text{m}$
$\lambda_3$	560	1.546 $\mu\text{m}$
$\lambda_4$	600	1.656 $\mu\text{m}$
$\lambda_5$	640	1.766 $\mu\text{m}$
$\lambda_6$	720	1.987 $\mu\text{m}$

The depth of field of our system varies from 1.27  $\mu\text{m}$  to 1.99  $\mu\text{m}$  and it provides a wide range of depth of field as compared to a monochromatic source which can be further extended using synthetic wavelengths by switching on two or more than two LEDs simultaneously.

### 3. Experimental Details

Fig.2 shows the schematic diagram of multi-spectral interference microscope (Nikon Eclipse LV100), in which we have replaced the halogen source with the synthesized light source made by commercially available cheap LEDs of different peak wavelengths. LEDs were mounted on a linear PCB board as shown in inset of Fig.2. The output power of individual LEDs is controlled by regulating the current flow. Since all the LEDs illuminate the diffuser in the common area, this diffused light is collected by the collecting lens and coupled to a multi-mode multiple fiber bundle as shown in the Fig.2. The light emerging from the output of fiber bundle was spatially incoherent with uniform intensity and uniform color distribution. Inset of the Fig.2 shows the schematic arrangement of the LEDs.

A Mirau-type interferometric objective (50X, NA=0.55) is used to achieve the interference in which a reference mirror and the beam-splitter ( $BS_2$ ) are embedded inside the microscope objective lens. LEDs are operated sequentially and light from each color LED is made incident onto the beam splitter ( $BS_1$ ) and then the reflected one passes through objective lens. The incoming light is again reflected by the inbuilt beam splitter ( $BS_2$ ) to the reference mirror and rest of the light is transmitted by  $BS_2$  towards the sample object.

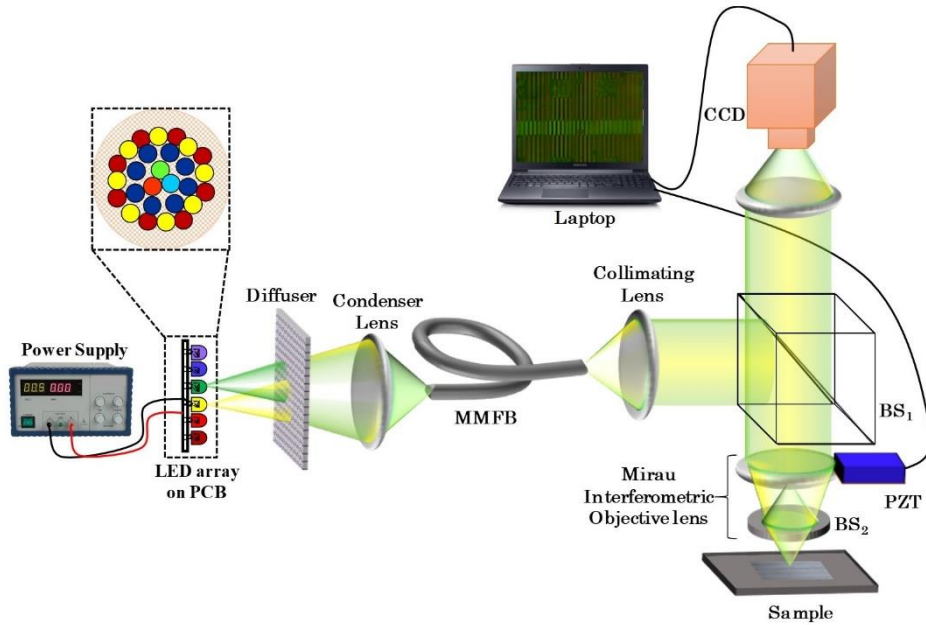


**Fig.2** Schematic diagram illustrating synthetic wavelength scanning interferometry with multi-color LED light source.

Interference takes place only when the two optical path lengths are equal and interference fringes can be observed, as far as the optical path difference introduced by the object step height is within the coherence length of the tuned light source. This microscope objective lens is attached to a piezo-electric transducer (PZT) (Piezo, Jena, MIPOS 3) to generate the phase shifted interferograms. The PZT is driven by an amplifier which is controlled by the computer, and it shifts the inbuilt reference mirror in vertical direction to generate the optical path difference and introduces the phase shift between the reference and object beams. Since vertical movement of the objective lens was less than the depth of focus of the objective lens; therefore, the sample remains within focus throughout the whole measurement. Phase-shifted color interferograms are stored in the computer for further processing.

#### 4. Results and discussion

Fig.3 shows the interferograms recorded by sequentially switching on the multi-color LEDs one by one listed in Table 1. The sample used to get the interference is a Si-IC chip. We can see the interference only in the region where the optical path difference (OPD) of the object and the reference beams are within the coherence length of each individual LED light sources.



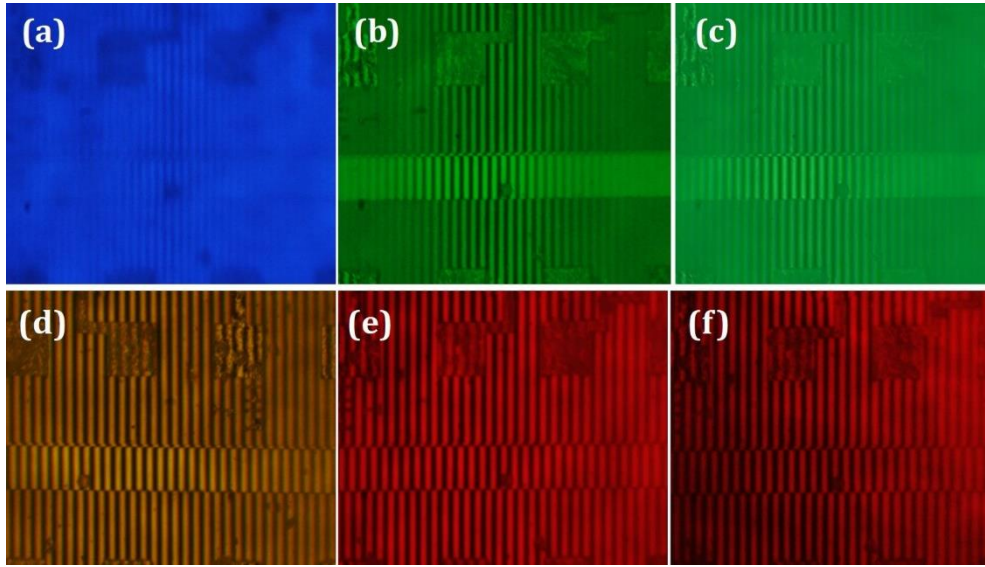


**Fig.3** Interferograms recorded by sequentially switching on multicolor LEDs (a)-(f) 460nm, 520nm, 560nm, 590nm, 640nm, and 720nm, respectively using Si-IC circuit as an object.

Further we have observed the formation of synthetic wavelength by illuminating the sample with two different wavelengths simultaneously. The usefulness of this technique is for the step like objects, so we demonstrated the experiments on Si-IC chip and a standard object. Smoothly varying surfaces (biological specimens) will not have the phase ambiguity as we can trace the deformation of fringes accordingly, so our technique is helpful for step height objects. Here we have performed the experiment on another similar object shown in Fig. 4 with a step height  $\sim 0.5 \mu\text{m}$ .

We have chosen a Si-IC chip with a step height  $\sim 0.5 \mu\text{m}$  for 3D surface profilometry as shown in Fig.4. This height generates an OPD of  $1 \mu\text{m}$  in reflection mode, which is much larger than the wavelength and it can incorporate ambiguity in height measurement. Fig.4 (a)-(d) shows one of the five phase-shifted interferograms and their reconstructed phase maps corresponding to 640 nm and 520 nm wavelengths. Fig.4 (c)-(d) shows the height profile of the step object corresponding to the black dotted line. It is observed from Fig.4 (e)-(f) that none of the line profiles shows the actual height of the specimen i.e.,  $0.5 \mu\text{m}$ . Further, to retrieve the actual height profile of the specimen phase subtraction method has been utilized as shown in Fig.4 (g). The measured height of the specimen is  $0.5 \pm 0.1 \mu\text{m}$ .

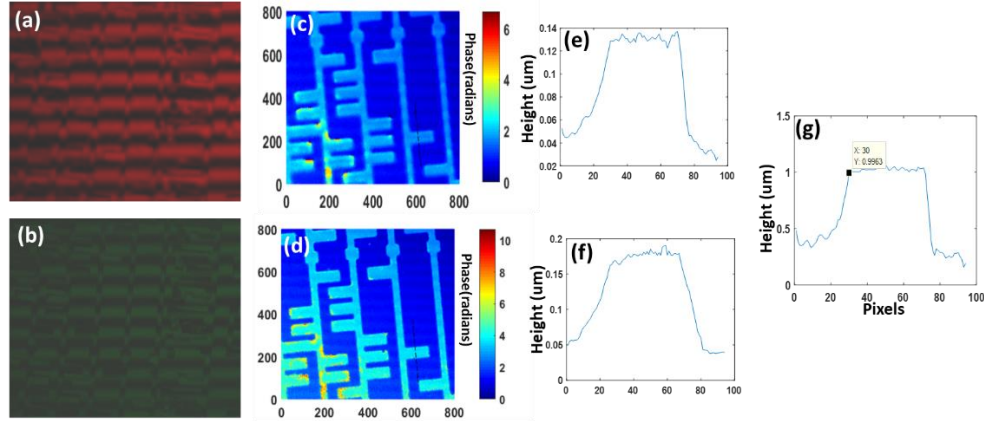


**Fig.4** Surface profilometry of Si-IC chip (a)-(b) One of the 5-phase shifted interferograms corresponding to 640nm and 520nm, respectively. (c)-(d) recovered phase map of the specimen using 5-phase shifted interferograms. (e)-(f) shows the recovered height profile of the specimen along the black dotted line. (g) Height profile of the sample using phase subtraction method

Fig.5 shows the formation of synthetic wavelength. Fig.5 (a)-(b) are the same interferograms corresponding to 520 nm and 640 nm wavelengths, respectively, as shown in Fig.3. Fig.5(c) show the formation of synthetic wavelength when both the light sources are switched on simultaneously. We can observe it by plotting the line profile of the interference pattern as shown in Fig.5 (d). The line profile shows the beat formation in the intensity distribution of the interference pattern due to synthetic wavelength which is otherwise not visible in individual interferogram.

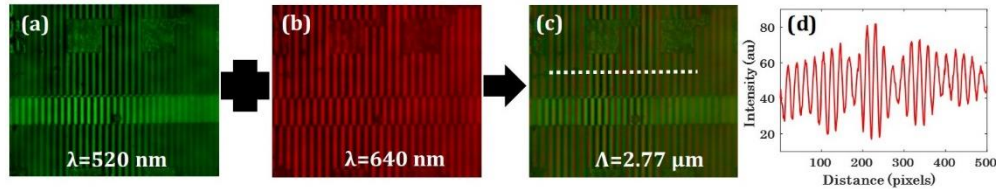


**Fig.5** Formation of synthetic wavelength using multicolor LEDs. (a)–(b) interferograms corresponding to 520nm and 640nm wavelengths, respectively. (c) interferogram corresponding to synthetic wavelength by illuminating the specimen with both wavelength light sources simultaneously. (d) line profile corresponding to white dotted line to visualize the formation of synthetic wavelength.

Since the coherence length of individual LED light sources are not significantly large to get high fringe density over whole field of view (FOV) as shown in Fig. 3 and 5. This reduces the space bandwidth product of the system and hence we cannot extract the quantitative information over whole FOV in single shot manner. Therefore, we have used phase shifting interferometry to extract the information of the specimen over full FOV. In Fig.6, we have demonstrated the capability of the present system. We have chosen a standard object with step height of 1  $\mu\text{m}$  for measurement of 3D surface topography. This height generates an OPD of 2  $\mu\text{m}$  in reflection mode, which is much bigger than the wavelength and hence an ambiguity will occur during height measurement. Fig.6 (a)-(b) shows one of the five phase shifted interferograms corresponding to 640 nm and 520 nm wavelengths, respectively. Fig.6 (c)-(d)

show the reconstructed phase maps of the structure over full FOV corresponding to 640nm and 520 nm wavelengths. The height profile of the step object is plotted corresponding to the red dotted line shown in Fig.6 (c)-(d). It is observed from Fig.6 (e)-(f) that none of the line profiles show the actual height of the specimen i.e., 1  $\mu\text{m}$ . This inaccuracy in the measurement occurs due to the ambiguity in the phase shift corresponding to OPD. Further, we have applied the phase subtraction method to recover the actual height profile of the specimen as shown in Fig.6 (g). The measured height of the specimen is  $1 \pm 0.1 \mu\text{m}$  which is very close to the actual height of the specimen.

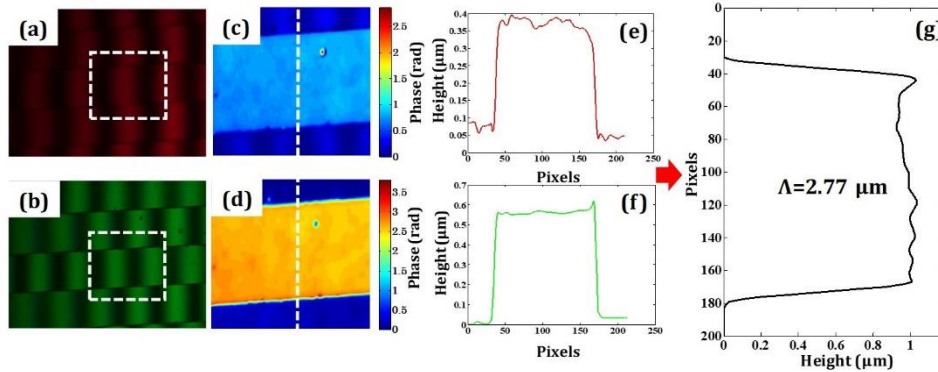


**Fig.6** Surface topography of the standard specimen. (a)-(b) One of the 5-phase shifted interferograms corresponding to 640nm and 520nm, respectively. (c)-(d) recovered phase map of the specimen using 5-phase shifted interferograms. (e)-(f) show the recovered height profile of the specimen along the white dotted line. (g) Height profile of the specimen using phase subtraction method.

Further, we have also measured the height of the specimen under observation using Stylus Profilometer. The height obtained from the profilometer matches well with the results obtained using our method. This shows the reliability of the proposed system. Our proposed system has advantage over the stylus profilometer that it can provide the areal topography measurement over whole FOV. It is fast, non-contact and provide accurate measurement.

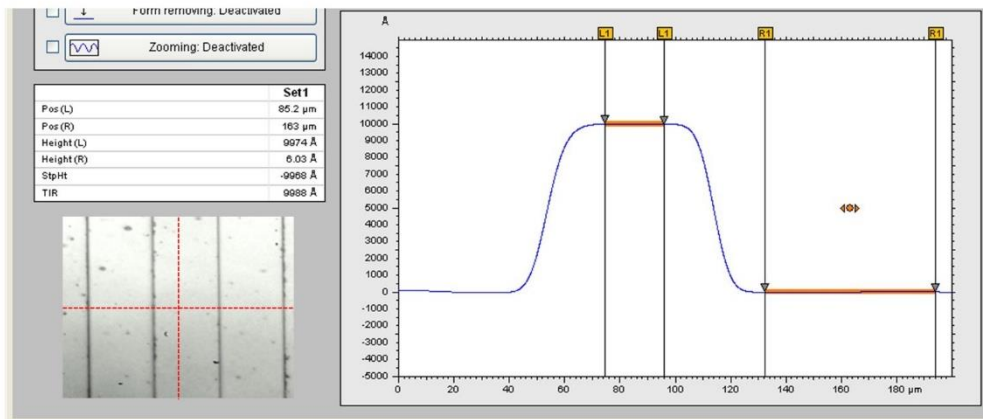


**Fig.7** Screenshot of the height measurement panel of stylus profilometer. The measured height is 9974  $\text{\AA}$ , which corresponds to 0.997 $\mu\text{m}$ .

## 5. Conclusion

Synthetic wavelength scanning interference based optical profilers are one of the best non-contact techniques for areal topographical measurement of various objects. Here, we successfully demonstrated the profilometry of a standard object having step height beyond the phase ambiguity using a synthesized multicolor LED light source. We are capable to provide a range of synthetic wavelengths  $\Lambda = \frac{\lambda_i \lambda_j}{\text{abs}[\lambda_i - \lambda_j]}$  using the proposed light source and hence we have extended range of height measurement within the coherence length range of the LEDs. The proposed light sources have low spatial and temporal coherence which reduces the possibility of speckle generation and multiple coherent reflections. This increases the signal to noise ratio of the proposed system. Here, we have used Mirau interferometer based objective lens which is a nearly common-path geometry, and it helps to enhance the phase sensitivity of the proposed system. By utilizing the phase shifting interferometry we have further reduced the measurement error. We have measured the height profile of a standard step like object and compared the results with Stylus profilometer. Our system is also capable to map the surface roughness of specimen over full FOV. In conclusion, we have developed a non-contact surface topography measurement system using commercially available multi-color LED light sources which can explore optical profiling as well as surface roughness measurement. The proposed system can be used in manufacturing environment by simply replacing the light source and microscope objective from any conventional bright-field microscope. The proposed system provides non-contact measurement which prevent any kind of contamination and damage to the sample surface under measurement. As per many developing countries low cost and easy accessibility are the major factors in technology transfer sectors. In addition, with the low-cost LED source, the proposed system utilises generation of multiple synthetic wavelengths, incoherent light source and phase shifting algorithm simultaneously which makes the system multi-modal and provides with full field multispectral extended range of height measurements.

## Acknowledgements:

The authors acknowledge the financial support provided by the University Grants Commission (UGC), New Delhi.

## Disclosure statement

No potential conflict of interest was reported by the author(s).

## References

- [1] G. E. Sommergren, "Optical heterodyne interferometry," *Appl. Opt.* **20**, 610-618 (1981).
- [2] K. Creath, "Phase-shifting interferometry techniques," in *Progress in Optics*, E. Wolf, ed. (Elsevier, New York, 1988), Vol. 26, pp. 357-373.
- [3] K. Creath, "Step height measurement using two-wavelength phase-shifting interferometry. *Appl. Opt.* 26, 2810-6 (1987).
- [4] B. S. Lee and T. C. Strand, "Profilometry with a coherence scanning microscope," *Appl. Opt.* **29**, 3784-3788 (1990).
- [5] P. J. Caber, "Interferometric profiler for rough surfaces," *Appl. Opt.* 32, 3438-3441 (1993).
- [6] T. Dressel, G. Hausler, and H. Venzke, "Three-dimensional sensing of rough surfaces by coherence radar," *Appl. Opt.* **31**, 919-925 (1992).
- [7] L. Deck, P. De Groot, "High-speed noncontact profiler based on scanning white light interferometry," *Appl. Opt.* **33**, 7334-7338 (1994).

- [8] M. Suematsu and M. Takeda, "Wavelength-shift interferometry for distance measurements using the Fourier transform technique for fringe analysis," *Appl. Opt.* 30, 4046-4055 (1991).
- [9] H. J. Tiziani, B. Franze, and P. Haible, "Wavelength-shift speckle interferometry for absolute profilometry using mode-hop free external cavity diode laser," *J. Mod. Opt.* 44, 1485-1496 (1997).
- [10] S. Kuwamura and I. Yamaguchi, "Wavelength scanning profilometry for real-time surface shape measurement," *Appl. Opt.* 36, 4473-4482 (1997).
- [11] T. H. Barnes, T. Eiju, and K. Matsuda, "Rough surface profile measurement using speckle optical frequency domain reflectometry with an external cavity tunable diode laser," *Optik* 103, 93-100 (1996).
- [12] A. Yamamoto, C. C. Kuo, K. Sunouchi, S. Wada, I. Yamaguchi, and H. Tashiro, "Surface Shape Measurement by Wavelength Scanning Interferometry Using an Electronically Tuned Ti:Sapphire Laser," *Opt. Rev.* 8, 59-63 (2001).
- [13] K. Hirabayashi, H. Tsuda, and T. Kurokawa, "Tunable wavelength-selective liquid-crystal filters for 600-channel FDM system," *IEEE Photon. Technol. Lett.* 4, 597-599 (1992).
- [14] H. Tsuda, K. Hirabayashi, T. Tohmori, and T. Kurokawa, "Tunable light source using a liquid-crystal Fabry-Perot interferometer," *IEEE Photon. Technol. Lett.* 3, 504-506 (1991).
- [15] D. S. Mehta, M. Sugai, H. Hinosugi, S. Saito, M. Takeda, T. Kurokawa, H. Takahashi, M. Ando, M. Shishido, and T. Yoshizawa, "Simultaneous three-dimensional step-height measurement and high-resolution tomographic imaging using spectral interferometric microscope," *Appl. Opt.* 41, 3874-3885 (2002).
- [16] D. S. Mehta, H. Hinosugi, M. Sugai, S. Saito, M. Takeda, T. Kurokawa, H. Takahashi, M. Ando, M. Shishido, and T. Yoshizawa, "A spectral interferometric microscope using tandem liquid-crystal Fabry-Perot interferometers for the extension of the dynamic range in three-dimensional step-height measurement," *Applied Optics*, 42 (4), 682-690 (2003).
- [17] D. S. Mehta, S. Saito, H. Hinosugi, M. Takeda, T. Kurokawa, "Spectral interference Mirau microscope with an acousto-optic tunable filter for three-dimensional surface profilometry" *Applied optics* 42 (7), 1296-1305 (2003).
- [18] S. K. Dubey, D. S. Mehta, A. Anand, C. Shakher, "Simultaneous topography and tomography of latent fingerprints using full-field swept-source optical coherence tomography," *Journal of Optics A: Pure and Applied Optics* 10 (1), 015307.
- [19] C. Polhemus, "Two-wavelength interferometry," *Appl. Opt.* 12, 2071-4 (1973).
- [20] Y. Y. Cheng, J. C. Wyant, "Two-wavelength phase shifting interferometry," *Appl. Opt.* 23, 4539 - 43 (1984).
- [21] J. Schmit, P. Hariharan, "Two-wavelength interferometry profilometry with a phase-step error-compensating algorithm," *Opt. Eng.* 45, 115602 (2006).
- [22] A. Nazarov, M. Ney and I. Abdulhalim, "Parallel spectroscopic ellipsometry system for fast correction of surface variability in metrology-based systems," *Novel Optical Systems Design and Optimization XXI* (Vol. 10746, p. 107460D). SPIE (2018).
- [23] S. Hua Lu and C. Chung Lee, "Measuring large step heights by variable synthetic wavelength interferometry", *Meas. Sci. Technol.* 13 (2002) 1382-1387
- [24] A. Aizen, M. Ney, A. Safrani and I. Abdulhalim, "A compact real-time high-speed high-resolution vibrometer, surface profiler and dynamic focus tracker using three wavelengths parallel phase-shift interferometry," *Optics and Lasers in Engineering*, 107, pp.304-314 (2018).
- [25] M. Ney, A. Safrani and I. Abdulhalim, "Three wavelengths parallel phase-shift interferometry for real-time focus tracking and vibration measurement," *Optics Letters*, 42(4), pp.719-722 (2013).
- [26] P. K. Upputuri, N. K. Mohan, and M. P. Kothiyal, "Measurement of discontinuous surfaces using multiple-wavelength interferometry," *Opt. Eng.* 48, 073603- 06 (2009).
- [27] Y. Y. Cheng, J. C. Wyant, "Multiple-wavelength phase-shifting interferometry," *Appl. Opt.* 24, 804-807 (1985).
- [28] R. Kuszmierz, J. Czarske and A. Fischer, "Multiple wavelength interferometry for distance measurements of moving objects with nanometer uncertainty", *Meas. Sci. Technol.* 25 (2014) 085202
- [29] A. Wada, M. Kato, Y. Ishii, "Large step-height measurements using multiple-wavelength holographic interferometry with tunable laser diodes," *J. Opt. Soc. Am. A Opt. Image Sci. Vis.* 25, 3013-20 (2008).
- [30] A. Nazarov, M. Ney and I. Abdulhalim, "Compact and fast sub-nm scale displacement probe using a phase mask and parallel phase-shift interferometry," *Journal of Physics D: Applied Physics*, 51(33), p.335102 (2018).

- [31] Y. Emery, T. Colomb and E. Cuhe, "Metrology applications using off-axis digital holography microscopy" *Journal of Physics: Photonics*, Volume 3 (2021).
- [32] P. Pavlíček, Erik Mikeska, "White-light interferometer without mechanical scanning," *Optics and Lasers in Engineering*, Volume 124,105800 (2020).
- [33] G. Xu, Y. Wang, S. Xiong, G. Wu, "Digital-micromirror-device-based surface measurement using heterodyne interferometry with optical frequency comb," *Applied Physics Letters* 118, 251104 (2021).
- [34] I. Abdulhalim, "Theory for double beam interference microscopes with coherence effects and verification using the Linnik microscope," *Journal of Modern Optics*, 48(2), pp.279-302 (2001).
- [35] I.Abdulhalim, M.Ney, A. Aizen, A. Nazarov, and A.Safrani, "Parallel phase shift microscopy, vibrometry and focus tracking," In *Optical Micro-and Nanometrology VII* (Vol. 10678, p. 106780P). SPIE.
- [36] P. K. Upputuri, M. Pramanik, K. M. Nandigana, M. P. Kothiyal, "Multi-colour microscopic interferometry for optical metrology and imaging applications," *Optics and Lasers in Engineering*, 84, 10–25 (2016).
- [37] T. Guo, F. Li, J.Chen, X. Fu, X. Hu, "Multi-wavelength phase-shifting interferometry for micro-structures measurement based on color image processing in white light interference," *Optics and Lasers in Engineering* 82 (2016) 41–47.
- [38] P. Mann, V. Singh, S. Tayal, P. Thapa, D. S. Mehta, "White light phase shifting interferometric microscopy with whole slide imaging for quantitative analysis of biological samples," *Journal of Bio photonics* (2022), 202100386.
- [39] V. Dubey, A. Ahmad, A. Butola, D. Qaiser, A. Srivastava, and D. S. Mehta, "Low coherence quantitative phase microscopy with machine learning model and Raman spectroscopy for the study of breast cancer cells and their classification," *Appl. Opt.* 58, A112-A119 (2019).
- [40] A. Ahmad, A. Kumar, V. Dubey, A. Butola, B. S. Ahluwalia, and D. S. Mehta, "Characterization of color cross-talk of CCD detectors and its influence in multispectral quantitative phase imaging," *Opt. Express* 27, 4572-4589 (2019).
- [41] I. Abdulhalim, and A. Safrani, "Real time parallel phase shift orthogonal polarization interference microscopy," In *Interferometry XVIII* (Vol. 9960, p. 996002). SPIE (2016)
- [42] A.Safrani and I. Abdulhalim, "High-speed 3D imaging using two-wavelength parallel-phase-shift interferometry," *Optics Letters*, 40(20), pp.4651-4654 (2015).
- [43] A. Pfortner & J.Schwider, "Red-green-blue interferometer for the metrology of discontinuous structures", *Applied Optics*, 42(4), 667 (2003).
- [44] A. T. Khmaladze, R. L. Matz, J. Jasensky, E. Seeley, M. M. Banaszak Holl, and Z. Chen, "Dual-wavelength digital holographic imaging with phase background subtraction," *Optical Engineering* 51(5), 055801 (2012).
- [45] A. Khmaladze, R.L. Matz, C. Zhang, T. Wang, M. M. Banaszak Holl, and Z. Chen, "Dual-wavelength linear regression phase unwrapping in three-dimensional microscopic images of cancer cells," *Opt. Lett.* 36, 912-914 (2011).
- [46] J. A. Izatt, M. A. Choma, "Theory of Optical Coherence Tomography", *Optical Coherence Tomography*, ISBN: 978-3-540-77549-2 (2008).
- [47] D. Malabari, "Interferometric Optical Profilers," *Optical Shop Testing*, 3rd Edition, Chapter15.4, pp. 698-699, John Wiley & Sons Inc.